J Solid State Electrochem (2008) 12:1567–1571
DOI 10.1007/s10008-008-0521-7

ORIGINAL PAPER

Deposition of Prussian blue on nanoporous gold film electrode and its electrocatalytic reduction of H_2O_2

Falong Jia · Chuanfang Yu · Jingming Gong · Lizhi Zhang

Received: 28 December 2007 / Revised: 20 January 2008 / Accepted: 21 January 2008 / Published online: 7 February 2008

Abstract Prussian blue-modified nanoporous gold film (PB-NPGF) electrode was fabricated in this study. The fabrication was realized through electrodeposition of Prussian blue nanoparticles on the skeleton of a nanoporous gold film electrode without destroying the porous structure of NPGF electrode. The resulting PB-NPGF composite electrode showed very high electrocatalytic activity, repeatability, and stability to the reduction of H_2O_2. For instance, its activity was about twenty times that of the PB-modified polished gold electrode. More importantly, the sensitivity of the PB-NPGF composite electrode reaches as high as 10.6 μA μM^{-1} cm^{-2}. This PB-NPGF composite electrode is very promising in the fields of catalysis, analysis, and so on.

Keywords Prussian blue · Nanoparticles · Nanoporous gold · Electrocatalytic activity · Electrodeposition

Abbreviations

PB	Prussian blue
NPGF	nanoporous gold film

Introduction

Prussian blue (PB) is well known for its wide applications in electrochromism [1, 2], photoresponse [3], electrocatalysis [4], sensors [5], and even batteries [6]. Since the first report on the synthesis of PB film by Neff [7], many methods have been reported, including casting from colloidal solution [8], Langmuir–Blodgett deposition [9, 10], and electrochemical deposition [11–13]. Among these methods, electrochemical deposition offers a convenient way to fabricate thin PB film on the conductive substrate. Moreover, to improve the analytical performances of deposited PB film, template-assisted technique was used to prepare nanostructured PB materials [14].

Detection of low levels of H_2O_2 is of great importance in enzymatic analysis and environmental control [15, 16]. Although many of the sensors based on the peroxidase could achieve high analytic sensitivity, the instability and high cost of peroxidase still hinder its wide application. PB is widely used in the biosensors for H_2O_2 and considered to be an "artificial enzyme peroxidase". The peculiar reduction product (Prussian white) in the cathodic process of PB is able to catalyze the electrochemical reduction of hydrogen peroxide at low potentials.

By now, PB films and nanoparticles have been deposited on a variety of surfaces, such as glassy carbon [14], platinum [17], gold [12], and carbon nanotube [18]. In our previous work, nanoporous gold film (NPGF) electrode with ultra high surface area was prepared by a convenient electrochemical alloying–dealloying process [19]. Compared with polished gold electrode, the NPGF electrode as the substrate could enhance electrochemical performance on the electrochemical detection and direction of methanol oxidation [20]. In this study, we used the NPGF as a skeleton for the electrodeposition of PB and evaluated the performance of the resulting PB-NPGF composite electrode on the reduction of H_2O_2. Compared with PB-modified polished gold electrode, the PB-NPGF electrode could greatly improve the responsive signal of H_2O_2 and effectively eliminate the interference from ascorbic acid and uric acid. To the best of our knowledge, this is the first

F. Jia (✉) · C. Yu · J. Gong · L. Zhang
Key Laboratory of Pesticide & Chemical Biology of Ministry of Education, College of Chemistry,
Central China Normal University,
Wuhan 430079, People's Republic of China
e-mail: fljia@mail.ccnu.edu.cn

report on the synthesis of Prussian blue-modified nanoporous gold film electrode and its electrocatalytic application.

Materials and methods

Materials All chemicals of analytical grade and gold wire (99.99%, 0.2 mm in diameter) were purchased from Shanghai Chemical Company. The solutions were prepared using deionized water (>18 MΩ cm).

Instrumentation The electrochemical experiments were performed on an electrochemical workstation (CHI660B, CHI Instruments, Shanghai). Field emission scanning electron microscopy (FESEM) was performed by using a scanning electron microscope (JEOL-6700F).

Methods The fabrication of NPGF electrode was conducted in a $ZnCl_2$/benzyl alcohol solution and the concentration of $ZnCl_2$ was 1.6 M [19]. Multi-cyclic electrochemical alloying–dealloying on gold electrode was realized in a three-electrode cell, which consisted of a Zn plate as auxiliary electrode, a Zn wire as reference electrode, and a gold wire as working electrode. The geometric area of gold electrode exposed to the electrolyte was 7.5 mm^2. Multi-cyclic potential sweep was applied to the working electrode at a scan rate of 10 mV s^{-1}. The first cycle should be in the sequence of open circuit→−0.72 V→1.88 V and the later cycles were from 1.88 V to −0.72 V, repeatedly. After 30 cycles, the gold electrode was taken out and cleaned quickly by benzyl alcohol, ethanol, and deionized water in sequence. For the preparation of PB-NPGF electrode, the as-synthesized NPGF electrode was immersed in a deoxygenated solution containing 2.5 mM $K_3[Fe(CN)_6]$, 2.5 mM $FeCl_3$, 0.1 M KCl, and 0.1 M HCl. The deposition of PB was performed in a three-electrode system with NPGF as the working electrode, platinum plate as the counter electrode, and a saturated calomel electrode (SCE) as the reference electrode, through 25 times of cyclic potential scans in the range of −0.2 to 0.6 V (vs. SCE) at 50 mV/s. After electrodeposition, the electrode was quickly rinsed with 0.01 M HCl solution and deionized water, respectively. For comparison, a polished gold wire was used for the deposition of PB with the same method. During the electrodeposition, only a 7.5-mm^2 area of the polished gold was exposed to the solution. All the electrochemical analysis were carried out at room temperature in a three-electrode cell, with the PB-NPGF as the working electrode, the Pt plate as the counter electrode, and SCE as the reference electrode. A certain concentration of H_2O_2 aqueous solution was prepared by adding H_2O_2 (30 wt.%) solution to pre-deoxygenated 0.1 M phosphate buffer solution (PBS, pH 6.0) containing 0.1 M KCl.

Results and discussion

Figure 1a shows the cyclic voltammetry curves of the polished gold electrode and the NPGF electrode, respectively, during the electrochemical deposition of PB. The cathodic peaks centered at 0.13 V corresponded to the reduction of PB to Prussian White, while the anodic peaks centered at 0.17 V referred to the oxidation of Prussian White to PB. It can be seen that the peak current continuously grew with the increase of scan times, indicating that the PB was gradually deposited on the electrodes. The peak current increased rapidly in the first several cycles and reached a constant value up to 25 cycles. This revealed that PB was fully covered on the electrodes at this time. So we chose 25 cycles of potential scans for the electrodeposition of PB for all the syntheses. Since the

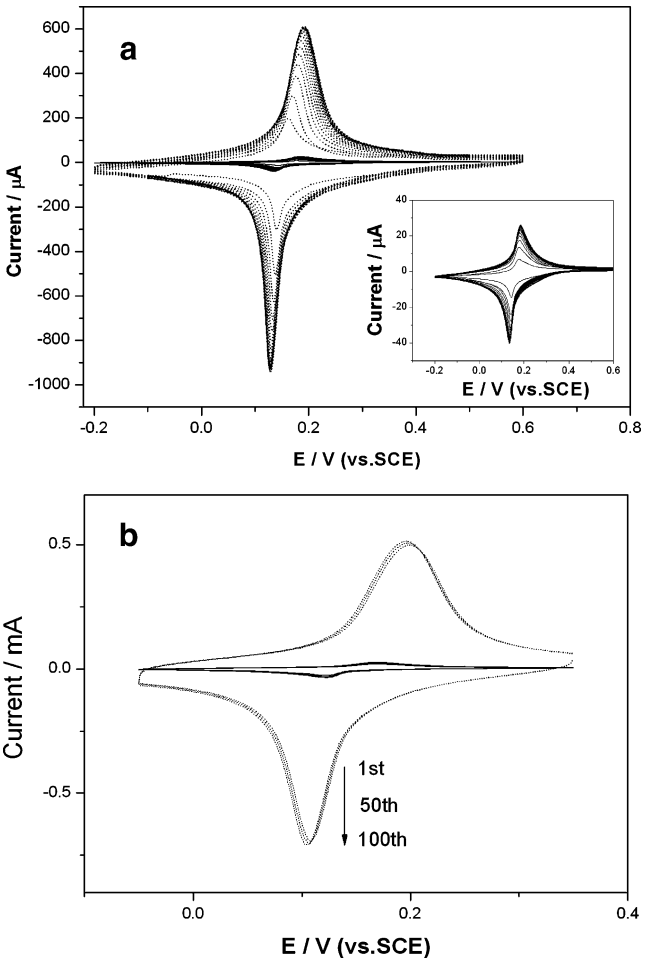

Fig. 1 **a** Cyclic voltammetry curves of a polished gold electrode (*solid line*) and NPGF electrode (*dotted line*) in a deoxygenated solution containing 2.5 mM $K_3[Fe(CN)_6]$, 2.5 mM $FeCl_3$, 0.1 M KCl and 0.1 M HCl. *Inset picture* is the magnified curves of polished gold. **b** Cyclic voltammetry curves of a PB-modified polished gold electrode (*solid line*) and a PB-NPGF electrode (*dotted line*) in a deoxygenated solution containing 0.1 M KCl and 0.1 M HCl at the *1st*, *50th*, and *100th* scans. Scan rate=50 mV s^{-1}

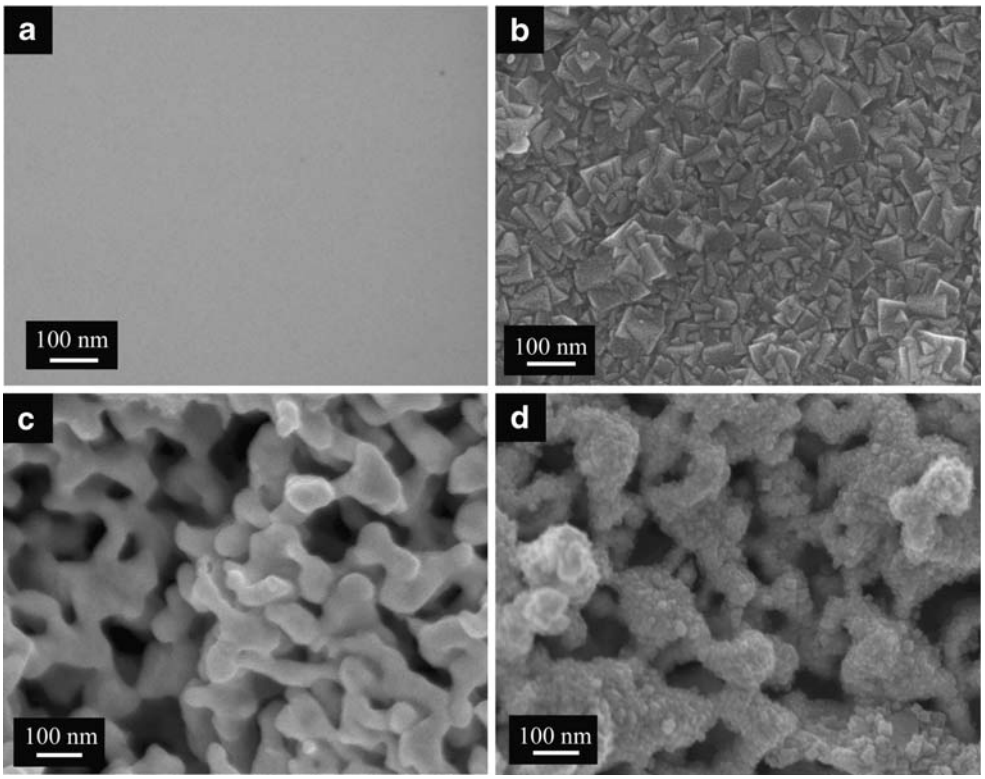

Fig. 2 FESEM images of gold electrodes before (**a**, **c**) and after (**b**, **d**) the electrodeposition of PB. **a**, **b** The polished gold electrode; **c**, **d** the NPGF electrode

charge under the cyclic voltammetry is directly associated with the amount of electroactive PB species, it was found that more amount of PB was deposited on the NPGF electrode than on the polished gold because the anodic peak current of NPGF was about twenty times higher than that of polished electrode.

The resulting as-prepared composite electrodes were transferred into the blank solution (0.1 M KCl and 0.1 M HCl) to test the stability of the deposited PB films by continuous cyclic potential scan from −0.05 V to 0.35 V vs. SCE. As seen from Fig. 1b, the redox peaks can be ascribed to the redox reaction of PB, confirming the presence of PB on the electrodes. Obviously, the redox peak current from the PB-NPGF electrode is much higher than that from the PB-modified polished gold one. With the continuous potential scan, the peak current decreased. The current loss was about 21% for the PB-modified polished gold electrode, whereas only 3% for that of the PB-NPGF electrode after 100 cycles. This high stability of the PB-NPGF electrode is very important for the application of PB

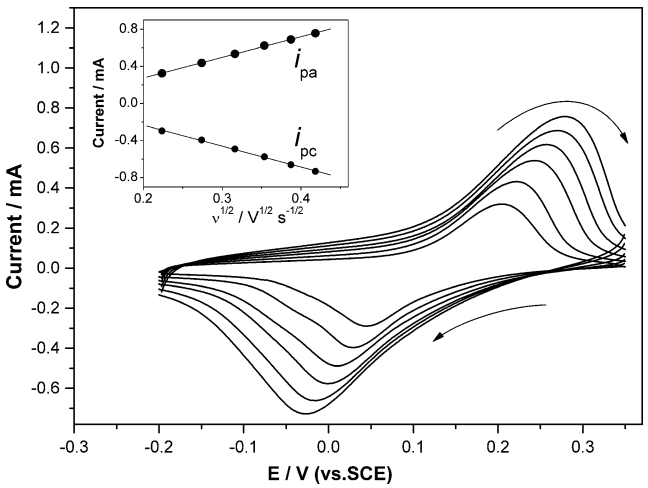

Fig. 3 Cyclic voltammetry curves of the PB-NPGF electrode in 0.1 M PBS (pH 6.0) containing 0.1 M KCl at different scan rates, from *inside* to *outside*: 50, 75, 100, 125, 150, and 175 $mV.s^{-1}$. The *inset* is the calibration plot of CV peak current versus square root of scan rate

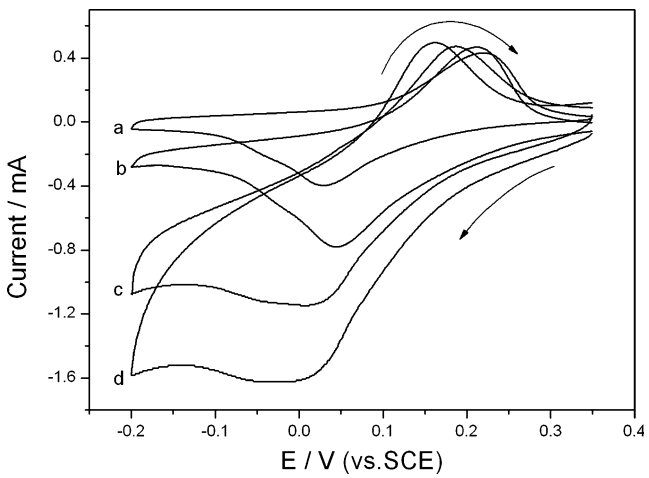

Fig. 4 Cyclic voltammetry curves of the PB-NPGF electrode in the 0.1 M PBS (pH 6.0) containing 0.1 M KCl. (*a*) in the absence of H_2O_2; (*b*) 0.1 mM H_2O_2.; (*c*) 0.2 mM; (*d*) 0.3 mM; starting potential was 0.35 V. Scan rate=75 $mV.s^{-1}$

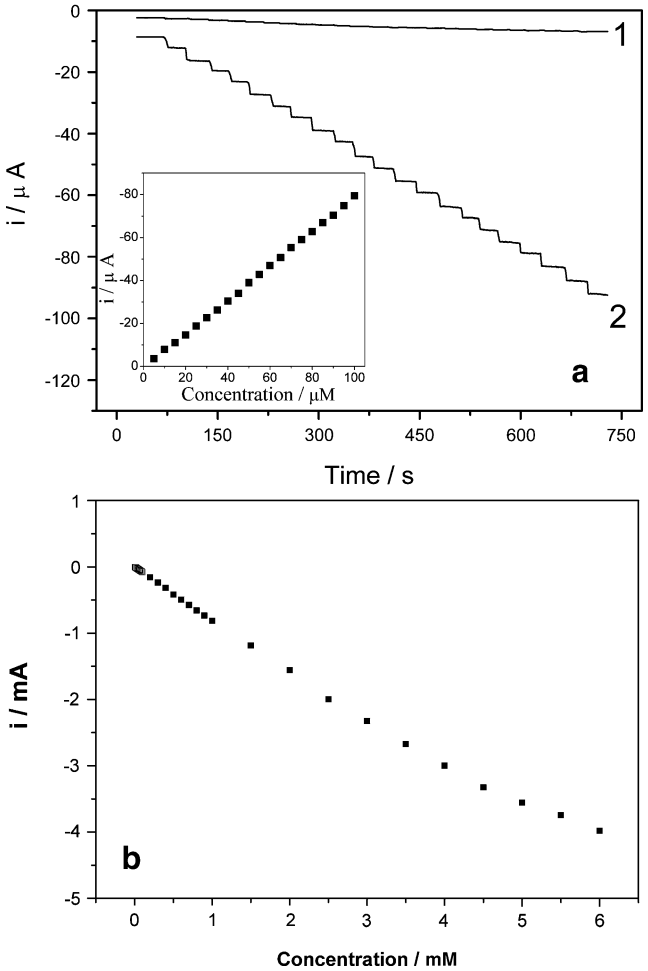

Fig. 5 **a** Amperometric response of PB-modified polished gold (*1*) and PB-NPGF (*2*) electrodes to successive injection of hydrogen peroxide into a stirring PBS solution (pH 6.0). The working potential was −0.05 V. The successive addition of hydrogen peroxide was 5 μM. The *inset* shows the calibration curve of hydrogen peroxide concentration at the PB/NPGF electrode (background current has been subtracted). **b** Response signal of PB-modified polished gold to H_2O_2 with successive addition of concentration at higher concentration

in analysis because the loss of activity would reduce its working life.

The morphologies of gold electrodes before and after PB electrodeposition are shown in Fig. 2. As shown in Fig. 2a and b, the PB nanoparticles with a size of ~70 nm were formed on the mirror-like polished gold surface. Figure 2c reveals that the as-synthesized NPGF electrode possesses nanoporous structure with a pore size of ~100 nm and ligament size of ~60 nm. Figure 2d clearly displays that PB nanoparticles have been successfully deposited on the ligaments of NPGF electrode. Compared with PB on the polished gold electrode (Fig. 2b), PB deposited on the NPGF electrode is of much smaller average size (~10 nm; Fig. 2d). Furthermore, the PB nanoparticles were uniformly distributed on the skeleton of NPGF and the porous structure of NPGF electrode remained well as compared with the original electrode (Fig. 2c).

The relationship between potential scan rate (v) and peak current (i_{pa}, i_{pc}) of PB-NPGF was investigated in the pH 6.0 PBS. In Fig. 3, it can be seen that the peak current, originating from the redox reaction between PB and Prussian White, increased accordingly with the scan rates increasing from 50 to 175 mV s^{-1}. The calibration plot (inset of Fig. 3) showed a good linear relationship between the peak current and the square root of the scan rate with a linear regression equation, $i_{pa}/\mu A = -0.169 + 2.22169 v^{1/2}/V\ s^{-1}$ (r=0.9996), and $i_{pc}/\mu A = 0.21836 - 2.26125\ v^{1/2}/V\ s^{-1}$ (r=−0.9992), respectively, indicating a diffusion-controlled process [21]. This linear relationship between peak current and $v^{1/2}$ was only valid in the scan rate range of 50 to 175 mV s^{-1}.

Figure 4 shows the cyclic voltammetry curves of the PB-NPGF electrode in the absence and presence of H_2O_2, respectively. In the absence of H_2O_2, the PB-NPGF electrode showed only signal of redox reaction from PB material. With the addition of H_2O_2 into solution, the cathodic peak was enhanced greatly at *ca.* −0.03 V vs. SCE, and gradually increased with the further addition of H_2O_2. This result indicated that the as-prepared PB-NPGF electrode showed high electrocatalytic activity towards the reduction of H_2O_2. To examine the sensitivity of PB-NPGF on the detection of H_2O_2, the amperometric response of PB-NPGF on H_2O_2 were measured in the stirring PBS solution. As shown in Fig. 5a, successive addition of H_2O_2 into the PBS results in a remarkable increase of reduction current. The increase was about twenty times that of the PB-coated polished gold electrode. The PB-NPGF electrode exhibited a rapid response within 5 s to reach the 90% steady-state response. The calibration plot (inset of Fig. 5) shows a good linear relationship with a correlation

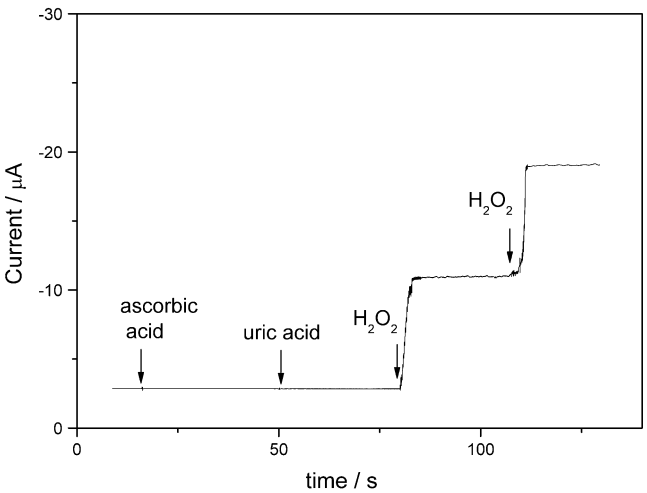

Fig. 6 Amperometric response of PB-modified polished gold electrode to *hydrogen peroxide* (10 μM) and different interferences (10 mM *ascorbic acid* and 10 mM *uric acid*) in a stirring PBS solution (pH 6.0). The working potential was −0.05 V

coefficient of 0.999 and a slope of 0.79 μA μM^{-1} (95% confidence, $i/\mu A = 0.94 - 0.79\ C/\mu M$). The detection limit was 2 μM on signal-to-noise ratio of 3. The corresponding sensitivity was 10.6 μA μM^{-1} cm^{-2}, which was much higher than other reports [14, 22]. Obviously, the three-dimensional porous structure and high surface area of NPGF as the skeleton makes a great contribution to the prominent performance with rapid response and high sensitivity. Figure 5b shows that the electrochemical response of PB to H_2O_2 is linear at the range of 0.005–3.5 mM. The reproducibility was investigated by measuring the current response for ten samples with the same concentration of 20 μM H_2O_2, and the relative standard deviation (RSD) is 2.2%. The stability of the PB-NPGF composite electrode was tested by measuring its response to 20 μM H_2O_2 after 1-month storage in PBS (pH 6.0), the loss of signal was only about 3%. It is reported that chromium(III) hexacyanoferrate-modified electrode exhibited high stability according to the detection of H_2O_2 [15]. This kind of material will be used to develop NPGF composite electrode with long-term stability in our further work.

It is known that there are some co-existing species, such as ascorbic acid and uric acid, in the body fluid of a real sample. These electroactive species may affect the response of hydrogen peroxide. Figure 6 shows the electrochemical signals of H_2O_2 at the PB-NPGF electrode under the interference of ascorbic acid and uric acid. These interference species brought negligible increase to the background current. The current increases for the two after addition of 10 μM H_2O_2 into the solution were 8.18 μA and 8.10 μA, respectively.

Conclusions

PB-NPGF composite electrode was fabricated by an electrochemical deposition method combined with a convenient alloying–dealloying process. PB nanoparticles were uniformly deposited on the skeleton of NPGF without blocking the porous structure of the electrode. The composite electrode showed higher electrocatalytic activity to the reduction of H_2O_2, which was about twenty times that of PB-modified polished gold electrode. The sensitivity of PB-NPGF composite electrode was as high as 10.6 μA μM^{-1} cm^{-2}. Meanwhile, the composite electrode possessed outstanding repeatability and stability. All the excellent performances of PB-NPGF composite electrode may be attributed to its three-dimensional porous structure and high surface area. This PB-NPGF composite electrode is very promising in the fields of catalysis and analysis.

Acknowledgments This work was supported by National Basic Research Program of China (973 Program; Grant 2007CB613301), National Science Foundation of China (Grants 20673041 and 20503009), Open Fund of Key Laboratory of Catalysis and Materials Science of the State Ethnic Affairs Commission & Ministry of Education, Hubei Province (Grants CHCL0508, CHCL06012, and CHCL07003).

References

1. Kulesza PJ, Miecznikowski K, Chojak M, Malik MA, Zamponi S, Marassi R (2001) Electrochim Acta 46:4371
2. Mortimer RJ (1993) Chem Soc Rev 26:147
3. Koncki R, Lenarczuk T, Glab S (2000) Anal Chim Acta 424:27
4. Pan KC, Chuang CS, Cheng SH, Su YO (2001) J Electroanal Chem 501:160
5. Zhao G, Feng JJ, Zhang QL, Li SP, Chen HY (2005) Chem Mater 17:3154
6. Jayalakshimi M, Scholz F (2000) J Power Sources 87:212
7. Neff VD (1978) J Electrochem Soc 125:886
8. Guo Y, Guadalupe AR (1999) Chem Mater 11:135
9. Qiu JD, Peng HZ, Liang RP, Li J, Xia XH (2007) Langmuir 23:2133
10. Zhao W, Xu JJ, Shi CG, Chen HY (2005) Langmuir 21:9630
11. Sato O, Lyoda T, Fujishima A, Hashimoto K (1996) Science 271:704
12. Zhang D, Wang K, Sun DC, Xia XH, Chen HY (2003) Chem Mater 15:4163
13. Ding Y, Gu G, Xia XH J Solid State Electrochem (2007) DOI 10.1007/s10008-007-0342-0
14. Karyakin AA, Puganova EA, Budashov IA, Kurochkin IN, Karyakina EE, Levchenko VA, Matveyenko VN, Varfolomeyev SD (2004) Anal Chem 76:474
15. de Lara Gonzalez GL, Kahlert H, Scholz F (2007) Electrochim Acta 52:1968
16. Wang Y, Huang J, Zhang C, Wei J, Zhou X (1998) Electroanalysis 10:776
17. Garjonyte R, Malinauskas A (1999) Sens Actuators B 56:93
18. Zou Y, S, un L, Xu F (2007) Talanta 72:437
19. Jia F, Yu C, Ai Z, Zhang L (2007) Chem Mater 19:3648
20. Yu C, Jia F, Ai Z, Zhang L (2007) Chem Mater 19:6065
21. Zakharchuk NF, Meyer B, Hennig H, Scholz F, Jaworsi A, Stojek Z (1995) J Electroanal Chem 398:23
22. Ricci F, Amine A, Palleschi G, Moscone D (2003) Biosens Bioelectron 18:165